# Uncertainty in ellipse fitting using a flatbed scanner: development and experimental verification

**J de Vicente[1], A M Sánchez-Perez[1], M Berzal[2], P Maresca[2] and E Gómez[2]**

[1] Departamento de Física Aplicada a la Ingeniería Industrial, Universidad Politécnica de Madrid, C/José Gutiérrez Abascal 2, E-28006 Madrid, Spain
[2] Departamento de Ingeniería Mecánica y Construcción, Universidad Politécnica de Madrid, Ronda de Valencia 3, E-28012 Madrid, Spain

E-mail: jvo@etsii.upm.es, amsanchez@etsii.upm.es, m.berzal@upm.es, piera.maresca@upm.es and emilio.gomez@upm.es

**Abstract**

In the field of dimensional metrology, the use of optical measuring machines requires the handling of a large number of measurement points, or scanning points, taken from the image of the measurand. The presence of correlation between these measurement points has a significant influence on the uncertainty of the result. The aim of this work is the development of an estimation procedure for the uncertainty of measurement in a geometrically elliptical shape, taking into account the correlation between the scanning points. These points are obtained from an image produced using a commercial flat bed scanner. The characteristic parameters of the ellipse (coordinates of the center, semi-axes and the angle of the semi-major axis with regard to the horizontal) are determined using a least squares fit and orthogonal distance regression. The uncertainty is estimated using the information from the auto-correlation function of the residuals and is propagated through the fitting algorithm according to the rules described in *Evaluation of Measurement Data—Supplement 2 to the 'Guide to the Expression of Uncertainty in Measurement'—Extension to any number of output quantities*. By introducing the concept of *cut-off length,* it can be observed how it is possible to take into account the presence of the correlation in the estimation of uncertainty in a very simple way while avoiding underestimation.

Keywords: optical dimensional metrology, correlation, measurement uncertainty, least square method, orthogonal distance, flatbed scanner, cut-off length

(Some figures may appear in colour only in the online journal)

## 1. Introduction

The use of a commercial scanner as a measuring instrument is common in various areas such as: engineering [1, 2], biology [3], archaeology [4], mineralogy [5] or cartography [6], thanks basically to the ease of image acquisition. In this work, a Canon PIXMA MP630 flat bed scanner has been used to obtain the images of the measurand. Prior to the image acquisition, the scanner was calibrated [7, 8], with the aim of gaining traceability from the corresponding primary standard. Measurement points are extracted from the images (figure 1). A black ellipse, drawn over a white plane, was scanned with the flat bed scanner using the standard software provided by the manufacturer (ScanGear ver. 14). A careful selection of the scanner parameters was made in order to get an image with enough contrast. The ellipse was scanned as a grayscale image (figure 1(*a*)) and stored using a non-compressed format (Windows Bitmap). The image was read using a MATLAB script and converted to a black and white image. Points of the ellipse border (measuring points) are those where a transition from black to white is observed (figure 1(*b*)).

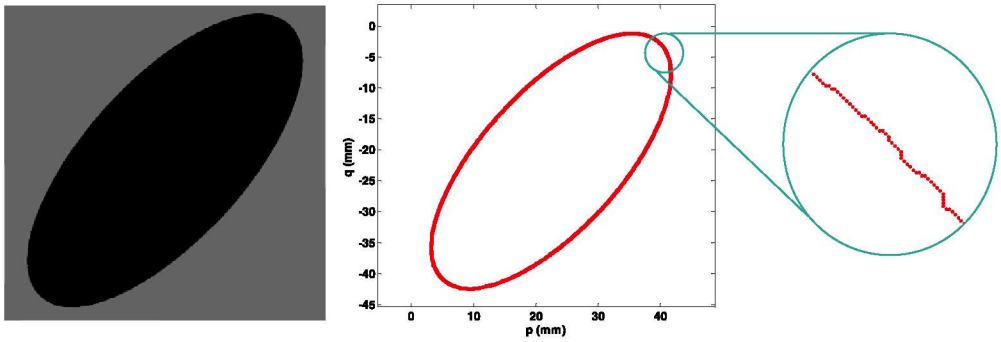


(*a*) (*b*)

**Figure 1.** Optical scanning of an ellipse: (*a*) ellipse obtained by the scanner, (*b*) edge of the ellipse and scanning points.

The extraction is carried out using a number of algorithms for the detection of edges [9]. One of the most widespread is the Canny [10], although, in this work, the 'thresholding' method [9, 11], has been used due to its easy implementation in order to simplify the presentation of the paper. Subsequently, the ellipse parameters and their corresponding uncertainties are estimated using the algorithms which are shown in section 2. In this paper, an elliptical shape is chosen because the ellipse is one of the simplest examples of quadratic curves (such as circumferences, parabolas and hyperbolas) or quadratic surfaces (spheres, ellipsoids, cylinders, cones, paraboloids, hyperboloids). So, the procedure described in this paper can easily be extended to cover all the geometrical features usually present in dimensional metrology: circumferences, ellipses, spheres, ellipsoids, cylinders and cones.

The need to use the correlation between the scanning points arises from the following basic statistical idea: suppose there are $x_1, x_2, \ldots, x_n$, $n$ statistically independent variables with the same standard uncertainty $u(x_i) = u_x$, if uncertainties were different the final result would be equivalent but the statistical analysis would be much more complicated; then, the uncertainty of the mean value $y = (x_1 + x_2 + \cdots + x_n)/n$ is $u(y) = u_x/\sqrt{n}$. If there is any correlation between these variables, the correlation coefficients are all equal to $r_{x_i,x_j} = r$, the uncertainty of their mean value is estimated using the following expression [12, 13]:

$$\begin{aligned}\mathrm{Var}(y) &= \mathrm{Var}\left(\frac{1}{n}\sum x_i\right) = \frac{1}{n^2}\mathrm{Var}\left(\sum x_i\right)\\ &= \frac{1}{n^2}\left(n\mathrm{Var}(x) + n(n-1)r\mathrm{Var}(x)\right)\\ u(y) &= u_x \cdot \sqrt{\frac{1-r}{n} + r} = \frac{u_x}{\sqrt{n_p}} \geqslant \frac{u_x}{\sqrt{n}}, \end{aligned} \tag{1}$$

where $n_p$ might be called '*effective number of variables*' or '*effective number of measuring points*' in coordinate metrology. This correlation effect can be taken into account in a very simple way: supposing that the mean value has been obtained from a number $n_p$, less than $n$, which are independent variables.

The influence of the correlation on the measurement uncertainty is significantly larger when the number of measuring points is high, (1). This is due to the following points.

- As will be seen in section 2.3, the correlation between scanning points is presented only when the distance between them is less than a certain *cut-off length* $\ell_c$. Therefore, if the number of scanning points is low and the mean distance between them is higher than $\ell_c$ either no correlation at all will appear, or its effect will be negligible. However, when the number of scanning points is very high, the mean distance between scanning points will be much less than the *cut-off length* $\ell_c$ and then, the correlation becomes significant.
- If the uncertainty estimation is carried out without taking the presence of correlation into account, the uncertainty expressions will appear to be divided by factor $\sqrt{n}$ instead of $\sqrt{n_p}$ (equation (1)). If $n$ is very high, the divisor $\sqrt{n}$ will cause the uncertainties to be clearly underestimated.

The aim of this paper is to make clear the presence of *correlation* between scanning points in coordinate metrology, and how this might significantly influence the measurement uncertainty. The correlation might be due to the presence of deviations introduced by the instrument at nearby scanning points, or due to the presence of irregularities in the piece to be measured, in which the evolution along the edge is not purely random but follows an almost deterministic rule, for example, the presence of lobes in the circular section of round parts such as drills.

## 2. Theoretical development

### 2.1. Determination of ellipse parameters by least squares

The ellipse is defined by the following *quadratic form*:

$$F(p, q) = ap^2 + 2bpq + cq^2 + 2dp + 2fq + g = 0, \tag{2}$$

where $(p, q)$ are the Cartesian coordinates belonging to the points on the ellipse, and $a$, $b$, $c$, $d$, $f$ and $g$ are the coefficients of the quadratic form. Once the $n$ scanning points are determined, there will be $n$ pairs of values $(p_i, q_i)$ which should cancel the expression $F(p_i, q_i) = 0$,

$$ap_i^2 + 2bp_iq_i + cq_i^2 + 2dp_i + 2fq_i + g \cong 0. \tag{3}$$

For the geometric characterization of the ellipse from the $n$ pairs of values $(p_i, q_i)$, it is necessary to estimate the components of the $\mathbf{y} = [a\,b\,c\,d\,fg]^{\mathrm{T}}$ vector.

The $(p_i, q_i)$ values come from measurements and have a non-negligible uncertainty, with the result that equations (3) are not exactly equal to zero[3]. The value of $g = 1$ is taken, in order to avoid the trivial solution, and to have a unique solution [14, 15].

Rewriting the foregoing equations using a matricial formalism: $\mathbf{A}_0$ represents the matrix of the coefficients of the coordinates $(p_i, q_i)$, $\mathbf{y}_0$ represents the vector of the coefficients of the quadratic form and $\mathbf{b}$ represents the column vector with the independent terms, and equation (3) is reduced to equation (4):

$$\begin{pmatrix} p_1^2 & 2p_1q_1 & q_1^2 & 2p_1 & 2q_1 \\ p_2^2 & 2p_2q_2 & q_2^2 & 2p_2 & 2q_2 \\ \vdots & \vdots & \vdots & \vdots & \vdots \\ \vdots & \vdots & \vdots & \vdots & \vdots \\ p_n^2 & 2p_nq_n & q_n^2 & 2p_n & 2q_n \end{pmatrix} \begin{pmatrix} a \\ b \\ c \\ d \\ f \end{pmatrix} \cong \begin{pmatrix} -1 \\ -1 \\ \vdots \\ \vdots \\ -1 \end{pmatrix} \tag{4}$$
$$\mathbf{A}_0\mathbf{y}_0 \cong \mathbf{b}.$$

The resolution of the system, equation (4), is carried out by means of an ordinary least squares fit, equation (5).

$$\mathbf{y} = (\mathbf{A}_0^{\mathrm{T}}\mathbf{A}_0)^{-1} \cdot \mathbf{A}_0^{\mathrm{T}}\mathbf{b}. \tag{5}$$

With this solution, $\mathbf{y}_0 = [a_0\,b_0\,c_0\,d_0\,f_0]^{\mathrm{T}}$, the sum of the squares of the residuals $e_i$ (sometimes called algebraic distances) is minimized, although this sum of squares does not have a geometric or metrological meaning. The variance of the residuals is estimated using the mean square error, equation (7):

$$e_i = ap_i^2 + 2bp_iq_i + cq_i^2 + 2dp_i + 2fq_i + 1. \tag{6}$$

$$s = \sqrt{\frac{1}{n-5}\sum_{i=1}^{n} e_i^2}. \tag{7}$$

The linear non-iterative procedure described in this subsection is simple but has some important limitations, such as its lack of robustness under certain circumstances [15, 16]. There are more methods that have robust behavior under an ill-conditioned data set [15]. The authors have chosen simplicity against robustness to reduce, as far as possible, the mathematical complexity of the paper. The algorithm described in this section is to provide an initial solution for the iterative procedure described in the next subsection.

### 2.2. Orthogonal regression

A better solution, from a metrological point of view, would be to minimize the orthogonal deviations $d_i$ from the measuring points to the fitted ellipse. These deviations are measured along the normal to the ellipse which passes through the measuring point being considered [17]:

$$d_i = \frac{F(p_i, q_i)}{|\nabla F|} = \frac{ap_i^2 + 2bp_iq_i + cq_i^2 + 2dp_i + 2fq_i + 1}{|\nabla F|}$$
$$\nabla F = \frac{\partial F}{\partial p_i}\mathbf{i} + \frac{\partial F}{\partial q_i}\mathbf{j} = (2ap_i + 2bq_i + 2d)\mathbf{i} + (2bp_i + 2cq_i + 2f)\mathbf{j}. \tag{8}$$

The vector gradient $\nabla F$ is a normal vector to the curve $F(p, q) = 0$. The deviations $d_i$ are a function of the solution selected $\mathbf{y} = [a\,b\,c\,d\,f]^{\mathrm{T}}$.

The orthogonal deviations $d_i$ have a clear geometrical meaning. On the other hand, algebraic distances of subsection 2.1 do not have a clear geometrical meaning. Moreover, orthogonal distances are the parameters commonly used in coordinate metrology to compute form defects.

Orthogonal $d_i$ deviations are linearized around the solution $\mathbf{y}_0 = [a_0\,b_0\,c_0\,d_0\,f_0]^{\mathrm{T}}$, equation (9):

$$d_i \cong d_{i0} + \frac{\partial d_i}{\partial a}\Delta a + \frac{\partial d_i}{\partial b}\Delta b + \frac{\partial d_i}{\partial c}\Delta c + \frac{\partial d_i}{\partial d}\Delta d + \frac{\partial d_i}{\partial f}\Delta f, \tag{9}$$

where $d_{i0}$ are the measurements with regard to the ellipse obtained in equation (5). Choosing the increment vector properly, $\Delta\mathbf{y}_1 = [\Delta a\,\Delta b\,\Delta c\,\Delta d\,\Delta f\,]^{\mathrm{T}} = \mathbf{y}_1 - \mathbf{y}_0$, it will be possible to make the deviations $d_i$ almost disappear:

$$0 \cong d_{i0} + \frac{\partial d_i}{\partial a}\Delta a + \frac{\partial d_i}{\partial b}\Delta b + \frac{\partial d_i}{\partial c}\Delta c + \frac{\partial d_i}{\partial d}\Delta d + \frac{\partial d_i}{\partial f}\Delta f, \tag{10}$$

$$\begin{bmatrix} \frac{\partial d_1}{\partial a} & \frac{\partial d_1}{\partial b} & \cdots & \frac{\partial d_1}{\partial f} \\ \frac{\partial d_2}{\partial a} & \frac{\partial d_2}{\partial b} & \cdots & \frac{\partial d_2}{\partial f} \\ \vdots & \vdots & \vdots & \vdots \\ \frac{\partial d_n}{\partial a} & \frac{\partial d_n}{\partial b} & \cdots & \frac{\partial d_n}{\partial f} \end{bmatrix} \cdot \begin{bmatrix} \Delta a \\ \Delta b \\ \Delta c \\ \Delta d \\ \Delta f \end{bmatrix} = \begin{bmatrix} -d_{10} \\ -d_{20} \\ \vdots \\ \vdots \\ -d_{n0} \end{bmatrix} \tag{11}$$
$$\mathbf{A}_1 \cdot \Delta\mathbf{y}_1 = -\mathbf{d}_0.$$

The solution of the system, $\mathbf{y}_1 = [a_1\,b_1\,c_1\,d_1\,f_1]^{\mathrm{T}}$, is obtained by iteratively minimizing the quadratic sum of the residuals of the system, equations (12) and (13):

$$\mathbf{y}_1 = \mathbf{y}_0 + \Delta\mathbf{y}_1 \tag{12}$$

$$\Delta\mathbf{y}_1 = -(\mathbf{A}_1^{\mathrm{T}}\mathbf{A}_1)^{-1} \cdot \mathbf{A}_1^{\mathrm{T}}\mathbf{d}_0. \tag{13}$$

The variance of the residuals is estimated using the mean quadratic deviation, $s_d$, equation (14):

$$s_d = \sqrt{\frac{1}{n-5}\sum_{i=1}^{n} d_i^2}. \tag{14}$$

Supposing that there is no correlation between the deviations $d_i$, and that these have the same uncertainty, the previous solution would be, according to the Gauss–Markov theorem, the *best linear unbiased estimator* of the true solution [18–20], and it is possible to estimate the *covariance matrix*

[3] For this reason, the '≅' symbol is used instead of the '=' symbol.

of $\mathbf{y}_1$: equation (15). From this it is possible to estimate the expanded uncertainties $U_{y_{1i}}$ of the components of $\mathbf{y}_1$ and the corresponding correlation coefficients $r_{y_{1i},y_{1j}}$, equations (16) and (17):

$$\mathbf{C}_{\mathbf{y_1}} = s_d^2 \cdot \left(\mathbf{A}_1^{\mathrm{T}}\mathbf{A}_1\right)^{-1}, \tag{15}$$

$$U_{y_{1i}} = k \cdot \sqrt{c_{y_{1i}}^2}, \tag{16}$$

$$r_{y_{1i},y_{1j}} = \frac{c_{y_{1i},y_{1j}}}{\sqrt{c_{y_{1i}}^2 \cdot c_{y_{1j}}^2}}, \tag{17}$$

where $c_{y_{1i}}^2$ is the $n$th term of the diagonal, $c_{y_{1i},y_{1j}}$ is a term which occupies the $(i, j)$ position in the matrix $\mathbf{C}_{\mathbf{y_1}}$ and $k$ is the overlap ratio.

The description of the ellipse in this way is not appropriate for subsequent use. For this reason, from the parameters $a$, $b$, $c$, $d$, $e$, $f$, the following are determined: the coordinates $(x_0, y_0)$ of the *center of the ellipse*; the *semi-major and semi-minor axes* $e_{\max}$, $e_{\min}$; and the *angle* $\theta$ that the *semi-major axis* makes with the horizontal axis, equation (18):

$$x_0 = \frac{cd - bf}{b^2 - ac}, \quad y_0 = \frac{af - bd}{b^2 - ac}, \quad \theta = \frac{1}{2}\cot^{-1}\left(\frac{a-c}{2b}\right)$$

$$e_{\max} = \sqrt{2\frac{af^2 + cd^2 + gb^2 - 2bdf - acg}{(b^2 - ac)\cdot\left[(c-a)\cdot\sqrt{1 + 2\left(\frac{b}{a-c}\right)^2} - (c+a)\right]}}$$

$$e_{\min} = \sqrt{2\frac{af^2 + cd^2 + gb^2 - 2bdf - acg}{(b^2 - ac)\cdot\left[(a-c)\cdot\sqrt{1 + 2\left(\frac{b}{a-c}\right)^2} - (c+a)\right]}}. \tag{18}$$

We define the vector $\mathbf{z}_1 = [x_0\, y_0\, e_{\max}\, e_{\min}\, \theta]^{\mathrm{T}}_{(y=y_1)}$, where $\mathbf{z}_1$ is a function of the vector $\mathbf{y}_1$, $\mathbf{z}_1 = \mathbf{H}(\mathbf{y}_1)$. Using the procedure described in supplement 2 of the GUM [21], the covariance matrix $\mathbf{C}_{\mathbf{z_1}}$ can be estimated by using the equation (19):

$$\mathbf{J} = \begin{bmatrix} \frac{\partial x_0}{\partial a} & \frac{\partial x_0}{\partial b} & \frac{\partial x_0}{\partial c} & \frac{\partial x_0}{\partial d} & \frac{\partial x_0}{\partial e} & \frac{\partial x_0}{\partial f} & \frac{\partial x_0}{\partial g} \\ \frac{\partial y_0}{\partial a} & \frac{\partial y_0}{\partial b} & \frac{\partial y_0}{\partial c} & \frac{\partial y_0}{\partial d} & \frac{\partial y_0}{\partial e} & \frac{\partial y_0}{\partial f} & \frac{\partial y_0}{\partial g} \\ \frac{\partial \theta}{\partial a} & \frac{\partial \theta}{\partial b} & \frac{\partial \theta}{\partial c} & \frac{\partial \theta}{\partial d} & \frac{\partial \theta}{\partial e} & \frac{\partial \theta}{\partial f} & \frac{\partial \theta}{\partial g} \\ \frac{\partial e_{a_0}}{\partial a} & \frac{\partial e_{a_0}}{\partial b} & \frac{\partial e_{a_0}}{\partial c} & \frac{\partial e_{a_0}}{\partial d} & \frac{\partial e_{a_0}}{\partial e} & \frac{\partial e_{a_0}}{\partial f} & \frac{\partial e_{a_0}}{\partial g} \\ \frac{\partial e_{b_0}}{\partial a} & \frac{\partial e_{b_0}}{\partial b} & \frac{\partial e_{b_0}}{\partial c} & \frac{\partial e_{b_0}}{\partial d} & \frac{\partial e_{b_0}}{\partial e} & \frac{\partial e_{b_0}}{\partial f} & \frac{\partial e_{b_0}}{\partial g} \end{bmatrix} \tag{19}$$

$$\mathbf{C}_{\mathbf{z_1}} = \mathbf{J}\cdot\mathbf{C}_{\mathbf{y_1}}\cdot\mathbf{J}^{\mathrm{T}}.$$

### 2.3. Determination of the autocorrelation

In the foregoing section, it is accepted, both for the calculation and for the estimation of the covariance matrix, (19), that there is no correlation in the orthogonal deviations $d_i$. Observing figures 2 and 3, the foregoing premise is not true, as for points situated a relatively small distance apart, the correlation is high: if a point has a positive deviation, the neighboring points generally also have a positive deviation.

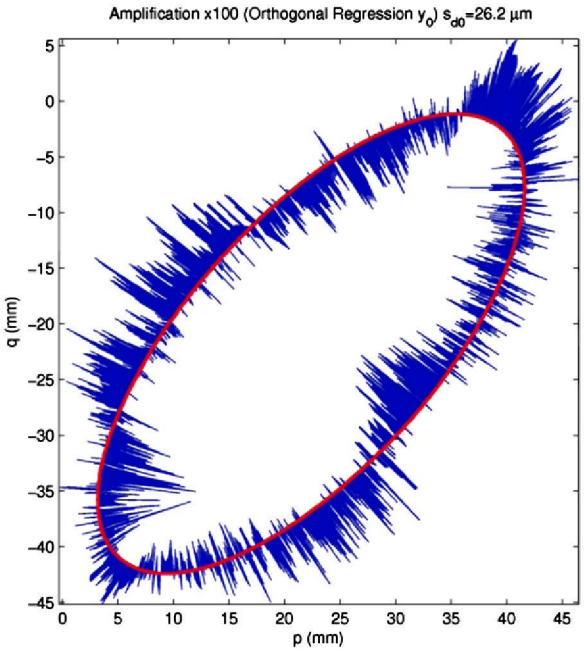


**Figure 2.** Orthogonal deviations $d_{i0}$.

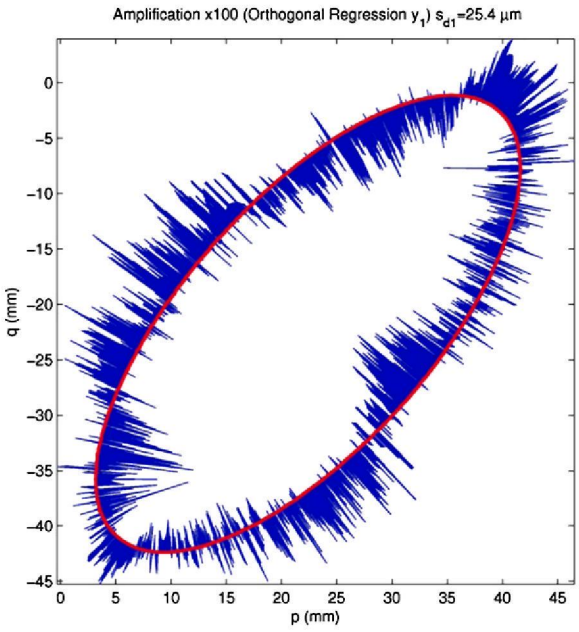


**Figure 3.** Orthogonal deviations $d_i$.

In order to verify the hypothesis of the independence of deviations $d_i$ the autocorrelation function is used [12, 22, 23]. The autocorrelation function shows the autocorrelation coefficients (20) as a function of the *lag*, figure 4:

$$r(k) = \frac{\sum_{i=k+1}^{n}(d_i - \bar{d})(d_{i-k} - \bar{d})}{\sum(d_i - \bar{d})^2}. \tag{20}$$

In figure 4 it is possible to see the variation of the correlation coefficient as a function of the *lag*. In order to simplify the determination of the covariance matrices, the line marked in black is taken as the function describing the evolution of the correlation coefficient versus the *lag*.

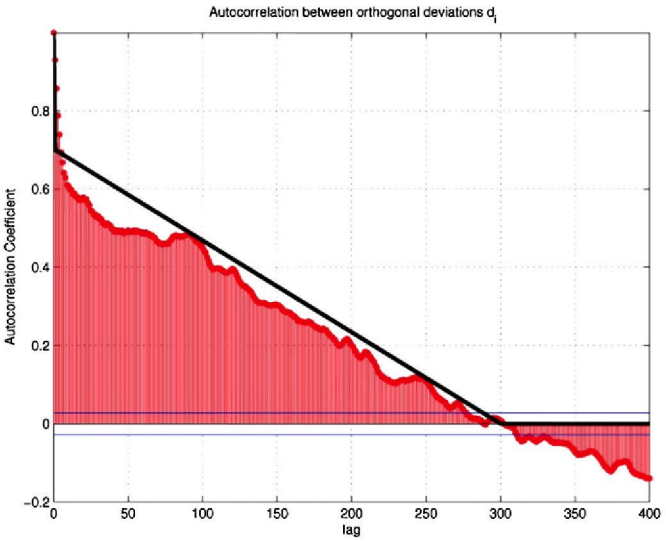


**Figure 4.** Autocorrelation function of the orthogonal deviations.

Taking the hypothesis $r_{d_i,d_j} = r$ where all the correlation coefficients are equal, the correlation matrix $\mathbf{C}_d$ will be:

$$\mathbf{C}_d = u^2[\mathbf{I} + r(\mathbf{I_1} - \mathbf{I})] = u^2 \begin{bmatrix} 1 & r & & r \\ r & 1 & & r \\ & & \ddots & \\ r & r & & 1 \end{bmatrix} = u^2\Gamma, \tag{21}$$

where $\mathbf{I_1}$ is the matrix of dimension $n \times n$ whose elements are 1, $\mathbf{I}$ is the identity matrix of dimension $n \times n$ and $u$ is the uncertainty of the independent variables.

By definition, the covariance matrix is positive definite and its eigenvalues have values greater than or equal to zero. In the previous conditions the eigenvalues of $\Gamma$ are:

$$\lambda_1 = \lambda_2 = \ldots = \lambda_{n-1} = 1 - r$$

$$\lambda_n = (n-1)r + 1.$$

Therefore $1 - r \geqslant 0$ which leads to $r \leqslant 1$ but also $(n-1)\,r + 1 \geqslant 0$ which leads to $r \geqslant -1/(n-1)$.

For $n = 2$, a pair of values, it is concluded that $r \geqslant -1$. For $n \gg 2$, as in the example of figure 1, $r = -1/(n-1) \simeq 0$. When there are many values of $x_i$, most of the values of $r\left(x_i, x_j\right)$ are positive or negative, but very close to zero. Only a minority of values are often negative clearly below zero. This can be possibly observed in the autocorrelation function, figure 4.

It can be observed that between *lag* = 0 and *lag* = 300 the correlation coefficient decreases in a nearly linear way from $r = 0.7$ at lag = 1 to zero at *lag* = 300. For lags higher than 300, the correlation is very low and a null correlation coefficient can be assumed. So, this black line can be mathematically described as follows:

$$r_{d_i,d_j} = \begin{cases} |i-j| < 300 & r = 0.7 \cdot \left(1 - \frac{\text{lag}}{300}\right) \\ |i-j| \geqslant 300 & r = 0 \end{cases}, \tag{22}$$

$$c_{d_i,d_j} = \begin{cases} i = j & c_{d_i}^2 = s_d^2 \\ i \neq j & c_{d_i,d_j} = s_d^2 \cdot r_{d_i,d_j} \end{cases}. \tag{23}$$

The covariance matrix of the orthogonal deviations, $\mathbf{C}_d$, is estimated using the correlation coefficients $r_{d_i,d_j}$, equation (22), and the estimation of the measurement variance, $s_d^2$, equation (14).

### 2.4. Generalized least squares

In the case of the presence of correlation, the sum of squares to minimize $Q_2$ is provided iteratively by equation (24) and the solution is determined by equation (25).

$$Q_2 = \mathbf{d}^{\mathrm{T}} \cdot [\mathbf{C}_d]^{-1} \cdot \mathbf{d}, \tag{24}$$

$$\Delta\mathbf{y}_2 = (\mathbf{A}_1^{\mathrm{T}} \cdot [\mathbf{C}_d]^{-1} \cdot \mathbf{A}_1)^{-1} \cdot \mathbf{A}_1^{\mathrm{T}} \cdot [\mathbf{C}_d]^{-1} \cdot \mathbf{d}_0, \tag{25}$$

$$s_Q = \sqrt{\frac{Q_2}{(n-m)}}. \tag{26}$$

The solution can be expressed as $\mathbf{y}_2 = \mathbf{y}_0 + \Delta\mathbf{y}_2$, together with its covariance matrix, $\mathbf{C}_{\Delta\mathbf{y}_2}$, equation (27):

$$\mathbf{C}_{\mathbf{y}_2} = \mathbf{C}_{\Delta\mathbf{y}_2} = (\mathbf{A}_1^{\mathrm{T}} \cdot [\mathbf{C}_d]^{-1} \cdot \mathbf{A}_1)^{-1}. \tag{27}$$

If the orthogonal distances $d_i$ are normally distributed, then $Q_2$ will be distributed according to a chi-squared distribution with $n - m$ degrees of freedom, with $m = 5$ being the number of parameters of the quadratic form to be determined. Therefore, the variable $s_Q$, which represents the mean quadratic error, (26), will possess an expected value equal to one [13, 18, 24]. The procedure of adjustment by generalized least squares (GLS), described in the foregoing manner, seems quite elegant and easy to implement. However, when it is analyzed in a little more detail, it is observed that it implies the inversion of the matrix $\mathbf{C}_{\mathbf{y}_{1C}}$ of dimensions $n \times n$, where $n$ is a very large number. This is not an easy task and requires a long processing time, and may also lead to high numerical errors which are in turn translated into the presence of significant numerical errors in $\mathbf{y}_2$.

### 2.5. Propagation of uncertainty using the orthogonal distance

If, for the estimation of uncertainties, it is necessary to carry out an adjustment by GLS, it will be necessary to invert the matrix $\mathbf{C}_d$. In order to avoid this, the matrix is propagated in the adjustment through *orthogonal regression*; that is to say, the matrix $\mathbf{C}_d$ is propagated through the said adjustment [24, 25]. The covariance matrix, $\mathbf{C}_{\mathbf{y}_3}$, is determined by applying the law of propagation of covariance matrices, equation (28):

$$\Delta\mathbf{y}_3 = -(\mathbf{A}_1^{\mathrm{T}}\mathbf{A}_1)^{-1} \cdot \mathbf{A}_1^{\mathrm{T}}\mathbf{d}_0 = \mathbf{M} \cdot \mathbf{d}_0, \tag{28}$$

$$\mathbf{C}_{\mathbf{y}_3} = \mathbf{M} \cdot \mathbf{C}_{\mathbf{d}} \cdot \mathbf{M}^{\mathrm{T}}. \tag{29}$$

The solution of the system is carried out by defining $\mathbf{z}_3 = [x_0\, y_0\, e_{\max}\, e_{\min}\, \theta]^{\mathrm{T}}_{(y=y_3)}$ and applying the transformation $\mathbf{z}_3 = \mathbf{H}(\mathbf{y}_3)$.

In order to propagate the calibration uncertainties to the ellipse parameters, it will be assumed that the fitting algorithm is the procedure described. Therefore, the combined covariance matrix $\mathbf{C}_{\mathbf{y}_3}^{(\mathrm{com})}$ of the ellipse parameters $\mathbf{y}_3$ would be:

**Table 1.** Results obtained with Matlab (uncertainty fitting component only).

| Ordinary LS | $a_0$ (mm$^{-2}$) | $b_0$ (mm$^{-2}$) | $c_0$ (mm$^{-2}$) | $d_0$ (mm$^{-1}$) | $f_0$ (mm$^{-1}$) | $s_0$ |
|---|---|---|---|---|---|---|
| | $7.4822 \times 10^{-4}$ | $-4.7565 \times 10^{-4}$ | $6.4861 \times 10^{-4}$ | $-2.71242 \times 10^{-2}$ | $2.47780 \times 10^{-2}$ | $5.5 \times 10^{-4}$ |
| Orthogonal regression | $a_1$ (mm$^{-2}$) | $b_1$ (mm$^{-2}$) | $c_1$ (mm$^{-2}$) | $d_1$ (mm$^{-1}$) | $f_1$ (mm$^{-1}$) | $s_1$ (mm) |
| | $7.4846 \times 10^{-4}$ | $-4.7564 \times 10^{-4}$ | $6.4895 \times 10^{-4}$ | $-2.71258 \times 10^{-2}$ | $2.47849 \times 10^{-2}$ | $2.5 \times 10^{-3}$ |
| | $U(a_1)$ (mm$^{-2}$) | $U(b_1)$ (mm$^{-2}$) | $U(c_1)$ (mm$^{-2}$) | $U(d_1)$ (mm$^{-1}$) | $U(f_1)$ (mm$^{-1}$) | – |
| | $0.0009 \times 10^{-4}$ | $0.0004 \times 10^{-4}$ | $0.0009 \times 10^{-4}$ | $0.00019 \times 10^{-4}$ | $0.00018 \times 10^{-4}$ | – |
| Change in variable orthogonal regression | $x_0$ (mm) | $y_0$ (mm) | $e_{\max}$ (mm) | $e_{\min}$ (mm) | $\theta$ (deg) | – |
| | 22.4084 | −21.7684 | 11.1900 | 25.8547 | −42.0140 | – |
| | $U(x_0)$ (mm) | $U(y_0)$ (mm) | $U(e_{\max})$ (mm) | $U(e_{\min})$ (mm) | $U(\theta)$ (deg) | – |
| | 0.0012 | 0.0012 | 0.0015 | 0.0031 | 0.0039 | – |
| Generalized LS | $x_0$ (mm) | $y_0$ (mm) | $e_{\max}$ (mm) | $e_{\min}$ (mm) | $\theta$ (deg) | – |
| | 22.4084 | −21.7684 | 11.1900 | 25.8547 | −42.0140 | – |
| | $U(x_0)$ (mm) | $U(y_0)$ (mm) | $U(e_{\max})$ (mm) | $U(e_{\min})$ (mm) | $U(\theta)$ (deg) | – |
| | 0.0162 | 0.0176 | 0.0142 | 0.0245 | 0.0533 | – |
| Propagation orthogonal regression | $x_0$ (mm) | $y_0$ (mm) | $e_{\max}$ (mm) | $e_{\min}$ (mm) | $\theta$ (deg) | – |
| | 22.4084 | −21.7684 | 11.1900 | 25.8547 | −42.0140 | – |
| | $U(x_0)$ (mm) | $U(y_0)$ (mm) | $U(e_{\max})$ (mm) | $U(e_{\min})$ (mm) | $U(\theta)$ (deg) | – |
| | 0.0165 | 0.0177 | 0.0145 | 0.0249 | 0.0550 | – |
| Cutting length | $x_0$ (mm) | $y_0$ (mm) | $e_{\max}$ (mm) | $e_{\min}$ (mm) | $\theta$ (deg) | – |
| | 22.4083 | −21.7683 | 11.1901 | 25.8549 | −42.0139 | – |
| | $U(x_0)$ (mm) | $U(y_0)$ (mm) | $U(e_{\max})$ (mm) | $U(e_{\min})$ (mm) | $U(\theta)$ (deg) | – |
| | 0.0143 | 0.0160 | 0.0127 | 0.0190 | 0.0453 | – |

$$\begin{aligned}\mathbf{C}_{\mathbf{y_3}}^{(\mathrm{com})} &= \mathbf{M}\cdot\left(\mathbf{C_d}+\mathbf{C}_{\mathbf{d}}^{(\mathrm{cal})}\right)\cdot\mathbf{M}^{\mathrm{T}}\\ &= \mathbf{M}\cdot\mathbf{C_d}\cdot\mathbf{M}^{\mathrm{T}}+\mathbf{M}\cdot\mathbf{C}_{\mathbf{d}}^{(\mathrm{cal})}\cdot\mathbf{M}^{\mathrm{T}}\\ &= \mathbf{C}_{\mathbf{y_3}}^{(\mathrm{fit})}+\mathbf{C}_{\mathbf{y_3}}^{(\mathrm{cal})}.\end{aligned} \tag{30}$$

Matrix $\mathbf{C_d}$ represents the uncertainty component of vector $\mathbf{d}$ (orthogonal distances) due exclusively to the fitting process and it is the covariance matrix estimated in subsection 2.3. Matrix $\mathbf{C}_{\mathbf{d}}^{(\mathrm{cal})}$ represents the uncertainty components of vector $\mathbf{d}$ due exclusively to the calibration of the scanner. The fitting process and the calibration of the scanner can be considered statistically independent processes, therefore the combined covariance matrix is simply the addition of matrices $\mathbf{C_d}$ and $\mathbf{C}_{\mathbf{d}}^{(\mathrm{cal})}$.

Matrix $\mathbf{C}_{\mathbf{y_3}}^{(\mathrm{fit})} = \mathbf{M}\cdot\mathbf{C_d}\cdot\mathbf{M}^{\mathrm{T}}$ represents the uncertainty components of ellipse parameters $\mathbf{y}_3$ due exclusively to the fitting process. Matrix $\mathbf{C}_{\mathbf{y_3}}^{(\mathrm{cal})} = \mathbf{M}\cdot\mathbf{C}_{\mathbf{d}}^{(\mathrm{cal})}\cdot\mathbf{M}^{\mathrm{T}}$ represents the uncertainty components of ellipse parameters $\mathbf{y}_3$ due exclusively to the calibration of the scanner.

In this paper, only the uncertainty component due to the fitting algorithms is estimated. The remaining uncertainty components may be estimated, as indicated in the literature [7, 26, 27], and will be added as in equation (30).

### 2.6. Use of the cut-off length

If subsets of points (figure 5) are chosen so that their elements are separated from one another on the *lag* or *cut-off length*, determined with the autocorrelation function, these sets will not be correlated and the procedure described in equations (12)–(14) will be applicable. The number of points per subset is $n_p \approx n/lag$; in this case the *lag* is equal to 300, and the number of the subset is $n_s \approx n/n_p$. Each subset is fitted to an ellipse, and the mean and standard deviations are subsequently calculated with the results of the $n_s$ subsets. As the expanded uncertainty of the mean values, it is possible to take the standard deviation multiplied by a coverage factor $k = 2$.

## 3. Experimentation

### 3.1. Materials

The measurement of the ellipse has been carried out by means of an optical instrument: a Canon PIXMA MP630 commercial scanner of a resolution of up to 4800 ppm and a working area of 216 × 297 mm. All the measurements have been taken with a resolution of 1200 ppm, with the aim of allowing a reasonable handling of the images obtained with the MATLAB software and the hardware: a PC with an i7 processor at 2.8 GHz, 8Gb of RAM and Windows 7 Professional 64-bit operating system.

### 3.2. Computer simulation

The ellipse is measured from $n = 5144$ scanning points, working with a resolution of 1200 dpi, equivalent to a pixel

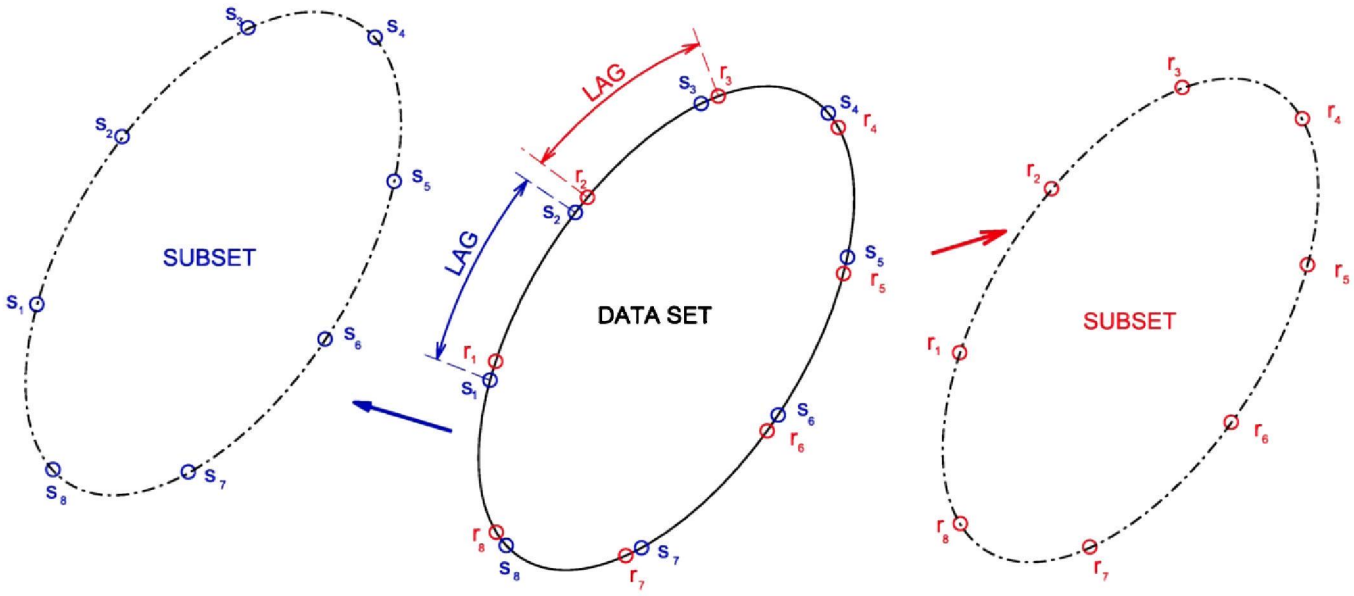


**Figure 5.** Use of the cut-off length or lag.

size of 21.2 $\mu$m. If there were no correlation between the points, the uncertainty of measurement would be proportional to $1/\sqrt{n} \approx 1/\sqrt{5144} \cong 0.014$. If correlation is present, the number of subsets is much smaller than the number of data; therefore $1/\sqrt{n_p} \approx 1/\sqrt{17} \cong 0.24$. This result is 17 times greater than the estimate based on the non-presence of correlation.

Using the equations (5) and (7), and the 5144 scanning points, the results of table 1, row Ordinary-LS, are obtained. This solution is considered to be the initial solution, $\mathbf{y_0} = [a_0, b_0, c_0, d_0, f_0]^{\mathrm{T}}$. $\mathbf{y_0}$ is modified using the orthogonal distance, equations (8)–(10) and (12), obtaining $\mathbf{y_1} = [a_1, b_1, c_1, d_1, f_1]^{\mathrm{T}}$, table 1, row orthogonal regression. The matrix of correlation coefficients for the solution $\mathbf{y}_1$ is reflected in equation (31):

$$\mathbf{R}_{\mathbf{y}_1} = \begin{bmatrix} 1 & -0.07 & -0.06 & -0.98 & -0.20 \\ -0.07 & 1 & -0.20 & +0.17 & -0.33 \\ -0.06 & -0.20 & 1 & +0.15 & +0.97 \\ -0.98 & +0.17 & +0.15 & 1 & +0.27 \\ -0.20 & -0.33 & +0.97 & +0.27 & 1 \end{bmatrix}. \quad (31)$$

Applying the transformation of equation (18), the solution $\mathbf{z}_1 = [x_0\, y_0\, e_{\max}\, e_{\min}\, \theta\,]^{\mathrm{T}}_{(y=y_1)}$ is calculated. The uncertainty associated with this new variable is determined by substituting in equation (19), obtaining the results from table 1, orthogonal regression with change of variable and the corresponding matrix of the correlation coefficients, equation (32):

$$\mathbf{R}_{\mathbf{z}_1} = \begin{bmatrix} 1 & +0.54 & +0.00 & -0.00 & -0.00 \\ +0.54 & 1 & +0.00 & -0.00 & +0.00 \\ +0.00 & +0.00 & 1 & +0.49 & +0.01 \\ -0.00 & -0.00 & +0.49 & 1 & +0.00 \\ -0.00 & +0.00 & +0.01 & +0.00 & 1 \end{bmatrix}. \quad (32)$$

The uncertainties obtained for $\mathbf{z}_1 = [x_0\, y_0\, e_{\max}\, e_{\min}\, \theta]^{\mathrm{T}}_{(y=y_1)}$ are in the order of micrometers, much smaller than the scale divisions of the instrument, 21.2 $\mu$m. This is in contradiction with the general recommendation in dimensional metrology, which indicates that uncertainties smaller than the scale division of the instrument should not be assigned or half a resolution at most should be assigned [28].

**Table 2.** Comparison of methods of adjustment.

| Method of adjustment | $s_Q$ | $Q_2$ |
|---|---|---|
| Ordinary LS | 1.005 60 | 5196.7 |
| Orthogonal regression | 1.005 33 | 5194.0 |
| Generalized LS | 1.005 72 | 5198.0 |

The analysis of correlation of the orthogonal distances is determined with the help of the autocorrelation function, and with the simplifications made to equations (22) and (23). The matrix $\mathbf{C_d}$ must be positive definite, as any covariance matrix. For this purpose, the maximum and minimum eigenvalues of the matrix are determined:

$$\lambda_{\max} = +(575.7\ \mu\mathrm{m})^2 \text{ and } \lambda_{\min} = +(0.5\ \mu\mathrm{m})^2.$$

These results prove that $\mathbf{C_d}$ is a positive definite matrix. The procedure of the generalized LS is described in equations (26)–(28). The inversion of a matrix of those dimensions is not an easy task: it requires a long processing time and, furthermore, it can involve the possibility of the presence of large numerical errors in $\mathbf{y}_2$. Determining the values of $s_Q$ and $Q_2$, equations (24) and (25), for the procedure of ordinary LS, for the orthogonal regression, and for generalized LS, the values of table 2 are shown.

The theoretical improvement introduced by the adjustment by GLS is totally compensated for by the numerical errors which appear in the inversion of the matrix $\mathbf{C_d}$, leading to worse adjustment results, $s_Q$ and greater $Q_2$, than those obtained through orthogonal regression, although the correlation was not taken into account. Therefore, the obtained $\mathbf{y}_2$ result would be of worse quality than the result $\mathbf{y}_1$ obtained by means of orthogonal regression. The estimation of uncertainties $\mathbf{U}_{\mathbf{y}_2}$ obtained in this way would be better, given that it takes the presence of correlation into account, than that obtained through orthogonal regression, which did not take the presence

**Table 3.** Comparison of the expanded uncertainties obtained.

| | | | | | | |
|---|---|---|---|---|---|---|
| | Orthogonal regression (OR) | $U(x_0)$ (mm) | $U(y_0)$ (mm) | $U(e_{\max})$ (mm) | $U(e_{\min})$ (mm) | $U(\theta)$ (deg) |
| | | 0.0012 | 0.0012 | 0.0015 | 0.0031 | 0.0039 |
| | Generalized LS (GLS) | $U(x_0)$ (mm) | $U(y_0)$ (mm) | $U(e_{\max})$ (mm) | $U(e_{\min})$ (mm) | $U(\theta)$ (deg) |
| | | 0.0162 | 0.0176 | 0.0142 | 0.0245 | 0.0533 |
| | Propagation orthogonal regression (POR) | $U(x_0)$ (mm) | $U(y_0)$ (mm) | $U(e_{\max})$ (mm) | $U(e_{\min})$ (mm) | $U(\theta)$ (deg) |
| | | 0.0165 | 0.0177 | 0.0145 | 0.0249 | 0.0550 |
| | Cut-off length (CL) | $U(x_0)$ (mm) | $U(y_0)$ (mm) | $U(e_{\max})$ (mm) | $U(e_{\min})$ (mm) | $U(\theta)$ (deg) |
| | | 0.0143 | 0.0160 | 0.0127 | 0.0190 | 0.0453 |
| COMP. 1 | GLS/OR | $\Delta U(x_0)$ | $\Delta U(y_0)$ | $\Delta U(e_{\max})$ | $\Delta U(e_{\min})$ | $\Delta U(\theta)$ |
| | | 14.0476 | 14.2669 | 9.2845 | 7.7817 | 13.5182 |
| COMP. 2 | GLS/PRO | $\Delta U(x_0)$ | $\Delta U(y_0)$ | $\Delta U(e_{\max})$ | $\Delta U(e_{\min})$ | $\Delta U(\theta)$ |
| | | 0.9852 | 0.9936 | 0.9792 | 0.9837 | 0.9681 |
| COMP. 3 | GLS/CL | $\Delta U(x_0)$ | $\Delta U(y_0)$ | $\Delta U(e_{\max})$ | $\Delta U(e_{\min})$ | $\Delta U(\theta)$ |
| | | 1.1354 | 1.0968 | 1.1138 | 1.2878 | 1.1753 |
| COMP. 4 | PRO/CL | $\Delta U(x_0)$ | $\Delta U(y_0)$ | $\Delta U(e_{\max})$ | $\Delta U(e_{\min})$ | $\Delta U(\theta)$ |
| | | 1.1524 | 1.1039 | 1.1375 | 1.3091 | 1.2140 |

of correlation into account. Therefore, $\mathbf{y_1}$, equation (12), is taken as a result accompanied by the estimation of uncertainties $\mathbf{U}_{\mathbf{y_2}}$, equation (27). The result $\mathbf{z}_2 = [x_0\, y_0\, e_{\max}\, e_{\min}\, \theta]^{\mathrm{T}}_{(y=y_2)}$ is defined using the transformation $\mathbf{z}_2 = \mathbf{H}(\mathbf{y}_2)$, table 1, row generalized LS. The corresponding matrix of correlation coefficients is therefore in the following form:

$$\mathbf{R}_{\mathbf{z}_2} = \begin{bmatrix} 1 & +0.56 & +0.05 & -0.01 & -0.03 \\ +0.56 & 1 & -0.00 & -0.00 & +0.01 \\ +0.05 & -0.00 & 1 & -0.27 & +0.05 \\ -0.01 & -0.00 & -0.27 & 1 & -0.01 \\ -0.03 & +0.01 & +0.05 & -0.01 & 1 \end{bmatrix}. \tag{33}$$

The propagation of the matrix $\mathbf{C_d}$ through orthogonal regression is carried out according to equations (28) and (29) obtaining $\mathbf{C}_{\mathbf{y_3}}$. Just as in the foregoing cases, a vector is defined $\mathbf{z}_3 = [x_0\, y_0\, e_{\max}\, e_{\min}\, \theta]^{\mathrm{T}}_{(y=y_3)}$ and the transformation is applied $\mathbf{z}_3 = \mathbf{H}(\mathbf{y}_3)$, table 1. The corresponding matrix of correlation coefficients is therefore in the following form:

$$\mathbf{R}_{\mathbf{z}_3} = \begin{bmatrix} 1 & +0.55 & +0.03 & -0.01 & -0.01 \\ +0.55 & 1 & 0.00 & 0.00 & +0.01 \\ +0.03 & 0.00 & 1 & -0.29 & +0.03 \\ -0.01 & 0.00 & -0.29 & 1 & 0.00 \\ -0.01 & +0.01 & +0.03 & 0.00 & 1 \end{bmatrix}. \tag{34}$$

The results are practically identical to those obtained with the adjustment by GLS, although the uncertainties are slightly greater: one tenth of a micrometer more in almost all cases. Nor are there significant differences in the correlation coefficients, equation (34), at most, a variation of 0.02. Therefore, it is verified that the procedure of propagation of the uncertainty matrix $\mathbf{C_d}$ through orthonormal regression leads to the same results obtained by means of an adjustment for GLS, but avoids the inversion of the matrix $\mathbf{C_d}$.

Finally, $n_s \approx n/n_p \approx 300$ subsets of points are taken in which there is no correlation. With these subsets, the vector $\mathbf{y}_0 = [a_0\, b_0\, c_0\, d_0\, f_0]^{\mathrm{T}}$, by means of ordinary LS, is determined for all the subsets. The vectors are subsequently determined by means of orthogonal regression $\mathbf{y_1} = [a_1, b_1, c_1, d_1, f_1]^{\mathrm{T}}$, and by making the corresponding transformation $\mathbf{z}_1 = [x_0\, y_0\, e_{\max}\, e_{\min}\, \theta]^{\mathrm{T}}_{(y=y_1)}$ for each subset. The most probable value for each of the parameters of $\mathbf{z}_1$ is the mean of the values of the subsets, and the expanded uncertainty is the coverage factor, $k = 2$, times the variance, table 1, row cut-off length; and the matrix of the correlation coefficients is:

$$\mathbf{R}_{\mathbf{z}_4} = \begin{bmatrix} 1 & +0.58 & -0.05 & -0.23 & +0.21 \\ +0.58 & 1 & -0.09 & -0.06 & +0.14 \\ -0.05 & -0.09 & 1 & -0.50 & -0.17 \\ -0.23 & -0.06 & -0.50 & 1 & -0.18 \\ +0.21 & +0.14 & -0.17 & -0.18 & 1 \end{bmatrix}. \tag{35}$$

## 4. Analysis of the results

There is a very large increase in the estimation of the uncertainties, the result of the presence of a strong correlation between scanning points, table 3 row COMP 1. This increase does not reach the 17 indicated above, but it is very high. This extreme value would be reached only if the correlation coefficient between scanning points lower than the *lag* had been exactly equal to one. Given that the variation of the said coefficient is linear, equation (22), the mean level of correlation is very low and, as a result, it is logical that the increase in uncertainty be less. For the case of the GLS, table 3, the uncertainties are greater than half of the instrument resolution, $21.2/2 = 10.6\,\mu$m, with the result that it would not be in contradiction with the usual rule in dimensional

metrology which indicates that *uncertainties of less than half the instrument resolution should not be assigned* [28].

A change in the sign of the correlation coefficient is also observed between the lengths of the semi-axes $e_{max}$ and $e_{min}$ in the orthogonal regression and in the GLS, which goes from being positive, +0.49 equation (32), to being negative, −0.27 equation (33); this has great importance in the estimation of the uncertainty associated with the difference in lengths between the semi-axes.

The uncertainties obtained in the case of the *cut-off length* are slightly lower than those obtained with the GLS and with propagation through orthogonal regression, between 10% for the center coordinate $y_0$ and 30% for the semi-minor axis $e_{min}$, table 3 rows COMP 3 and COMP 4. Despite these variations, they can be considered to be consistent estimations, in comparison with those obtained by ordinary LS and orthogonal regression in which the correlation was not taken into account.

In the case of correlation coefficients, equations (33)–(35), the differences are a little greater in the case of the *cut-off length*, above all in those coefficients in which $x_0$ or $\theta$ appears.

In this particular example, uncertainties coming from the fitting are significantly higher than those coming from calibration or due to thermal expansion. Combined uncertainties are only slightly higher than those coming from the fitting. Because of this, the influence of correlation in the combined uncertainties is very high. Probably, in a different situation, working with a bigger measurand of size three times higher, covering a big part of the calibrated measuring area of the scanner, calibration uncertainty components would be similar to those coming from fitting and the influence of correlation would be still present but its importance would not be so high.

## 5. Conclusions

This paper makes clear how the presence of correlation between measurement points can lead, when their number is very high, something usual in optical metrology, to significant underestimation of the measurement uncertainty.

A procedure has been described to show the presence of this correlation and to take it into account when estimating the parameters describing the measured geometrical element, an ellipse in the present example, and above all, when estimating the uncertainty of these parameters.

Also, it has been shown how to take into account the presence of this correlation during the uncertainty estimation through the introduction of a critical separation between points, the *cut-off length*, making unnecessary the use of complex algorithm such as generalized least squares.

## Acknowledgments

This work has been carried out within the DPI2008-01351 project, financed by the Spanish Government's National Industrial Design and Innovation Plan (Plan Nacional de Diseño e Innovación Industrial).

## References

[1] Kee C and Ratnam M 2009 A simple approach to fine wire diameter measurement using a high-resolution flatbed scanner *Int. J. Adv. Manuf. Technol.* **40** 940–7

[2] Korin I, Larrainzar C and Ipiña J P 2008 Crack length and stable crack extension measurements from images acquired by means of a conventional flatbed scanner *Fatigue Fract. Eng. Mater. Struct.* **31** 876–84

[3] van Dalen G 2004 Determination of the size distribution and percentage of broken kernels of rice using flatbed scanning and image analysis *Food Res. Int.* **37** 51–8

[4] Miriello D and Crisci G 2006 Image analysis and flatbed scanners a visual procedure in order to study the macro-porosity of the archaeological and historical mortars *J. Cult. Herit.* **7** 186–92

[5] Tarquini S and Armienti P 2003 Quick determination of crystal size distributions of rocks by means of a color scanner *Image Anal. Stereology* **22** 27–34

[6] Baltsavias E P and Waegli B 1996 Quality analysis and calibration of DTP scanners *Int. Arch. Photogramm. Remote Sens. B1* **31** 14–9

[7] de Vicente J, Sánchez M A, Gómez E and Barajas C 2011 Construction of a two-coordinates measuring machine from a commercial scanner *MESIC 2011: Proc. Int. Conf. of 4th Manuf. Eng. Soc. (Cadiz, Spain, 21–23 Sept.)*

[8] Kangasrääsiö J and Hemming B 2009 Calibration of a flatbed scanner for traceable paper area measurement *Meas. Sci. Technol.* **20** 107003

[9] Gonzalez R C, Woods R E and Eddins S L 2009 *Digital Image Processing Using MATLAB* (Upper Saddle River, NJ: Prentice-Hall)

[10] Canny J 1986 A computational approach to edge detection *IEEE Trans. Pattern Anal. Mach. Intell.* **PAMI-8** 679–98

[11] Rodger G 2001 Dimensional measurement using vision systems *Measurement Good Practice Guide No 39* (Teddington, UK: National Physical Laboratory)

[12] Peña D 2001 *Fundamentos de Estadística* (Madrid: Alianza Editorial)

[13] Taylor J R 1997 *An Introduction Error Analysis: The Study of Uncertainties in Physical Measurements* (Sausalito, CA: University Science Books)

[14] Kanatani K and Rangarajan P 2011 Hyper least squares fitting of circles and ellipses *Comput. Stat. Data Anal.* **55** 2197–208

[15] Fitzgibbon A W, Pilu M and Fisher R B 1999 Direct least-squares fitting of ellipses *IEEE Trans. Pattern Anal. Mach. Intell.* **21** 476–80

[16] Gander W, Golub G H and Strebel R 1994 Least-square fitting of circles and ellipses *BIT* **43** 558–78

[17] Joon Ahn S, Rauh W and Warnecke H 2001 Least-squares orthogonal distances fitting of circle, sphere, ellipse, hyperbola, and parabola *Pattern Recognit.* **34** 2283–303

[18] Björck A 1996 *Numerical Methods for Least Squares Problem* (Philadelphia, PA: SIAM)

[19] Pavese F and Forbes A B 2009 *Data Modeling for Metrology and Testing in Measurement Science* (Boston, MA: Birkhäuser)

[20] Plackett R 1950 Some theorems in least squares *Biometrika* **37** 149–57

[21] Bureau International des Poids et Mesures (BIPM), International Electrotechnical Commission (IEC), International Federation of Clinical Chemistry (IFCC), International Laboratory Accreditation Cooperation (ILAC), International Organization for Standardization (ISO), International Union of Pure and Applied Chemistry (IUPAC), International Union of Pure and Applied Physics (IUPAP) and International Organization of Legal Metrology

(OIML) 2011 *Evaluation of Measurement Data—Supplement 2 to the 'Guide to the Expression of Uncertainty in Measurement'—Extension to any number of output quantities* (Sèvres, France: BIPM) www.bipm.org/en/publications/guides/gum.html JCGM 102:2011

[22] Peña D 2005 *Análisis de Series Temporales* (Madrid: Alianza Editorial)

[23] Hamilton J 1994 *Time Series Analysis* (Princeton, NJ: Princeton University Press)

[24] Lira I 2002 *Evaluating the Measurement Uncertainty: Fundamentals and Practical Guidance* (London: Taylor and Francis)

[25] Bureau International des Poids et Mesures (BIPM), International Electrotechnical Commission (IEC), International Federation of Clinical Chemistry (IFCC), International Laboratory Accreditation Cooperation (ILAC), International Organization for Standardization (ISO), International Union of Pure and Applied Chemistry (IUPAC), International Union of Pure and Applied Physics (IUPAP) and International Organization of Legal Metrology (OIML) 2008 *Evaluation of Measurement Data—Guide to the Expression of Uncertainty in Measurement* (Sèvres, France: BIPM) www.bipm.org/en/publications/guides/gum.html JCGM 100:2008

[26] de Vicente J and Royo C 2012 Trazabilidad en la verificación de tamices mediante técnicas ópticas *e-medida Revista Española de Metrología* No. 1 Febrero 2012 pp 51–62 www.e-medida.es/hemerotecan4#!prettyPhoto

[27] de Vicente J, Sánchez-Pérez A M and Hernández W 2011 Virtual instruments in dimensional metrology *Proc. Research in Engineering Education Symp. (REES 2011) (Madrid, Spain, 4–7 October 2011)*

[28] European Co-operation for Accreditation 1999 EA-4/02 *Expression of the Uncertainty of Measurement in Calibration* (Paris: European Co-operation for Accreditation)